

Spectroscopic Study of δ Electron Transfer between Two Covalently Bonded Dimolybdenum Units via a Conjugated Bridge

Chun Y. Liu,* Xuan Xiao, Miao Meng, Yu Zhang and Mei Juan Han

Department of Chemistry, Jinan University, Guangzhou 510632, P. R. China.

Department of Chemistry, Tongji University, Shanghai 200092, P. R. China.

Supporting Information

Contents

Page S-2:

Figure S1. Vis-Near-IR spectra of the neutral dimolybdenum dimers.

Figure S2. Vis-Near-IR-mid-IR spectra of $\{[\text{Mo}_2(\text{DAniF})_3]_2(\mu\text{-O}_2\text{CC}_6\text{H}_4\text{CO}_2)\}\text{PF}_6$.

Page S-3:

Figure S3. Vis-Near-IR-mid-IR spectra of $\{[\text{Mo}_2(\text{DAniF})_3]_2(\mu\text{-OSCC}_6\text{H}_4\text{COS})\}\text{PF}_6$.

Figure S4. Vis-Near-IR-mid-IR spectra of $\{[\text{Mo}_2(\text{DAniF})_3]_2(\mu\text{-S}_2\text{CC}_6\text{H}_4\text{CS}_2)\}\text{PF}_6$.

Page S-4:

Figure S5. Vis-Near-IR-mid-IR spectra of $\{[\text{Mo}_2(\text{DAniF})_3]_2(\mu\text{-O}_2\text{CC}_6\text{H}_4\text{CS}_2)\}\text{PF}_6$.

Figure S6. CV of $\text{Mo}_2(\text{DAniF})_3(\mu\text{-S}_2\text{CC}_6\text{H}_5)$.

Page S-5:

Figure S7. DPV of $\text{Mo}_2(\text{DAniF})_3(\mu\text{-S}_2\text{CC}_6\text{H}_5)$.

Figure S8. CV of $\text{Mo}_2(\text{DAniF})_3(\mu\text{-O}_2\text{CC}_6\text{H}_5)$.

Figure S9. DPV of $\text{Mo}_2(\text{DAniF})_3(\mu\text{-O}_2\text{CC}_6\text{H}_5)$.

Page S-6:

Table S1. Electronic coupling matrix elements from Mulliken-Hush equation.

Page S-7:

Table S2. Effective energy gaps (ΔE_{ML}^{eff}) and effective coupling constants (H_{ML}^{eff}) for metal to ligand transition.

Table S3. Effective energy gaps (ΔE_{LM}^{eff}) and effective coupling constants (H_{LM}^{eff}) for ligand to metal transition.

Page S-8:

Table S4. Comparison between H_{ab} from Hush model and $H_{MM'}$ from CNS model.

Table S5. Electron transfer kinetics for the symmetrical complexes based on the electronic coupling matrix elements from Hush and CNS methods.

Page S-9:

Table S6. Electron transfer kinetics for the unsymmetrical complexes based on the electronic coupling matrix elements from CNS methods.

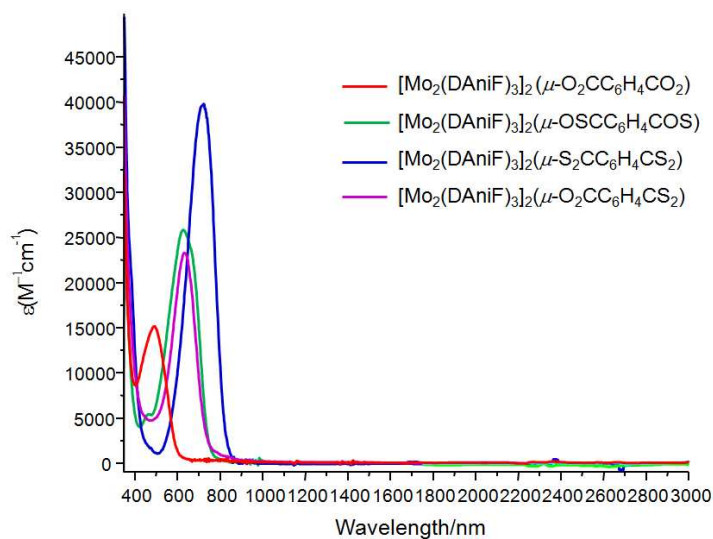


Figure S1. Vis-Near-IR spectra of the neutral dimolybdenum dimers, recorded in the CH_2Cl_2 solutions at room temperature.

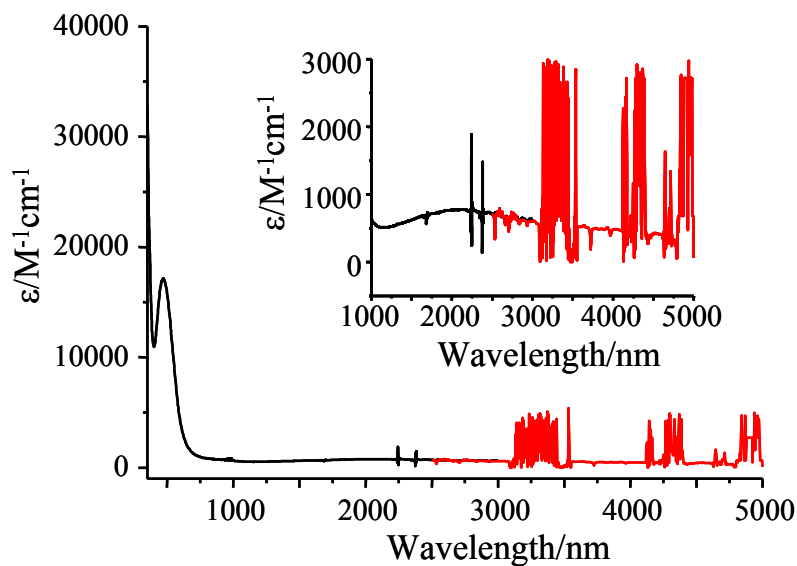


Figure S2. Combined Vis-Near-IR (black) and IR spectra (red) for $\{[\text{Mo}_2(\text{DAniF})_3]_2(\mu\text{-O}_2\text{CC}_6\text{H}_4\text{CO}_2)\} \text{PF}_6$ in CH_2Cl_2 solution at room temperature.

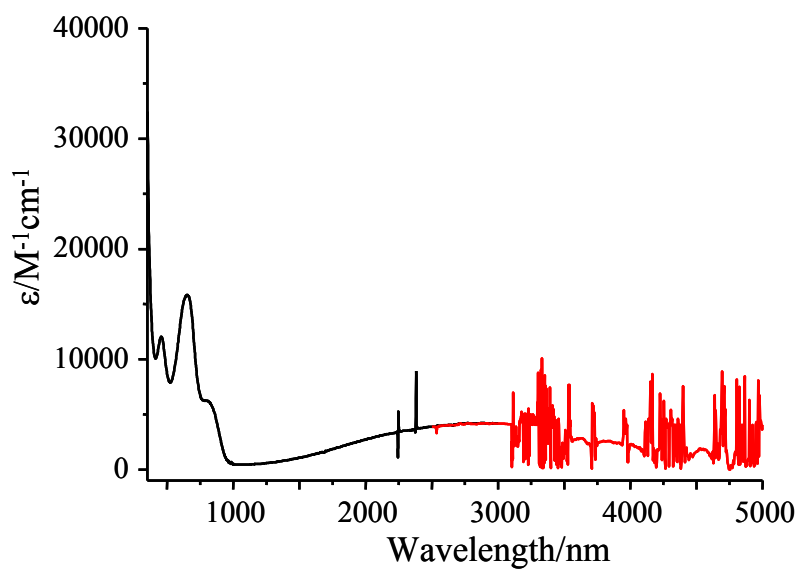


Figure S3. Combined Vis-Near-IR (black) and IR spectra (red) for $\{[\text{Mo}_2(\text{DAniF})_3]_2(\mu\text{-OSCC}_6\text{H}_4\text{COS})\}\text{PF}_6$ in CH_2Cl_2 solution at room temperature.

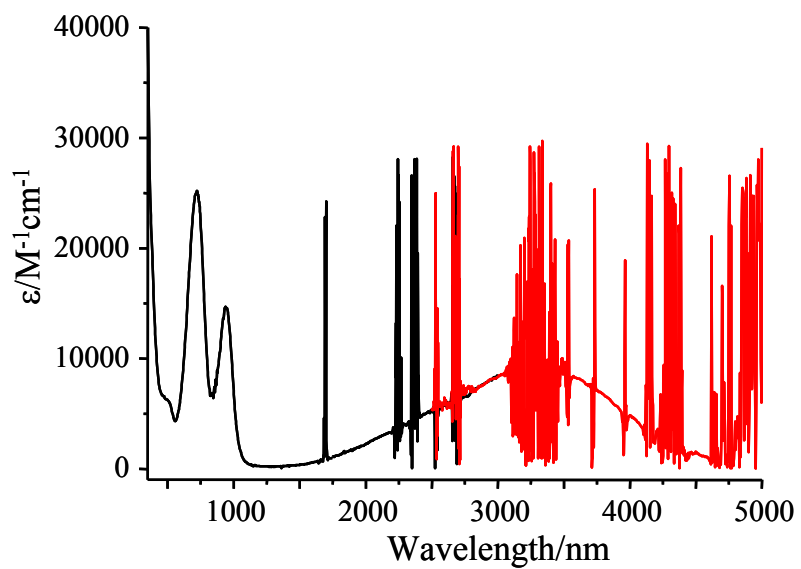


Figure S4. Combined Vis-Near-IR (black) and IR spectra (red) for $\{[\text{Mo}_2(\text{DAniF})_3]_2(\mu\text{-S}_2\text{CC}_6\text{H}_4\text{CS}_2)\}\text{PF}_6$ in CH_2Cl_2 solution at room temperature.

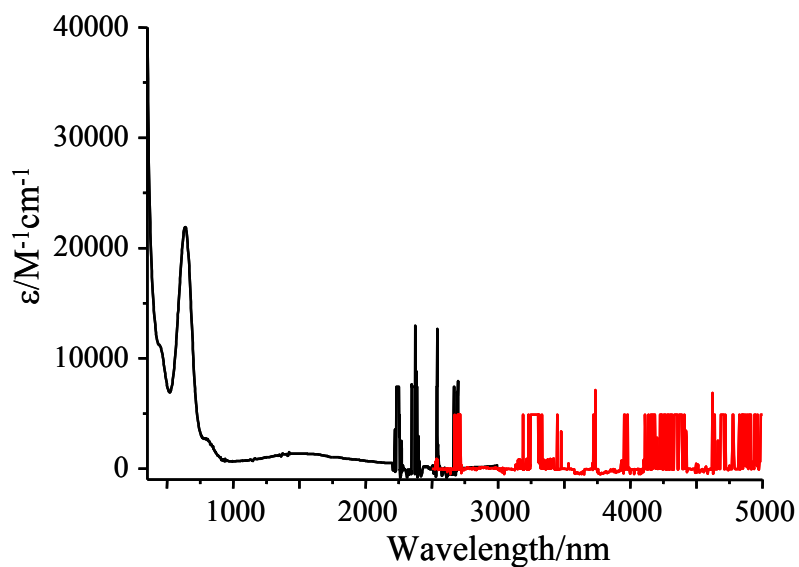


Figure S5. Combined Vis-Near-IR (black) and IR spectra (red) for $\{[\text{Mo}_2(\text{DAniF})_3]_2(\mu\text{-O}_2\text{CC}_6\text{H}_4\text{CS}_2)\}\text{PF}_6$ in CH_2Cl_2 solution at room temperature.

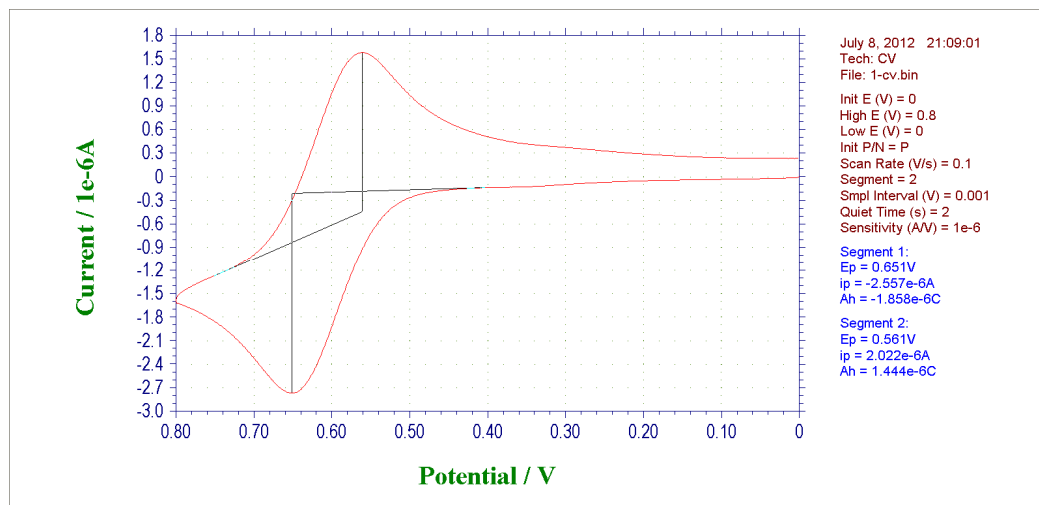


Figure S6. CV of $\text{Mo}_2(\text{DAniF})_3(\mu\text{-S}_2\text{CC}_6\text{H}_5)$. $E_{\text{ox}} = 0.651 \text{ V}$, $E_{\text{red}} = 0.561 \text{ V}$ (vs Ag/AgCl).

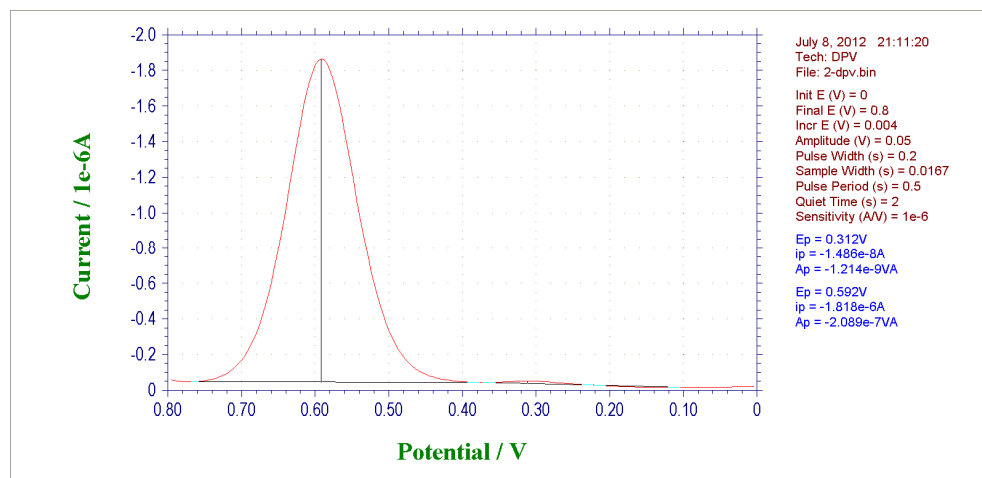


Figure S7. DPV of $\text{Mo}_2(\text{DAniF})_3(\mu\text{-S}_2\text{CC}_6\text{H}_5)$. Half-wave potential $E_p = 0.592\text{ V}$ (vs Ag/AgCl)

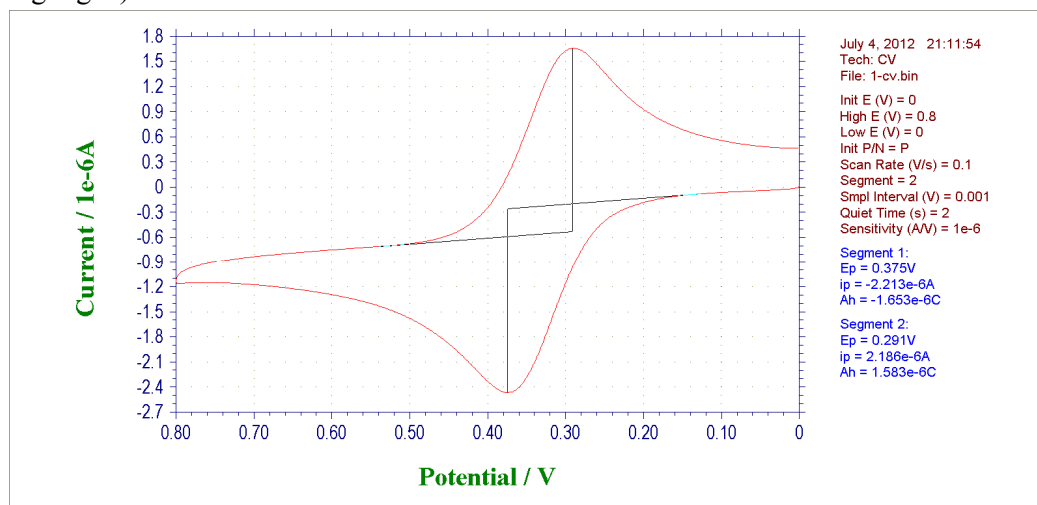


Figure S8. CV of $\text{Mo}_2(\text{DAniF})_3(\mu\text{-O}_2\text{CC}_6\text{H}_5)$. $E_{ox} = 0.375\text{ V}$, $E_{red} = 0.291\text{ V}$ (vs Ag/AgCl)

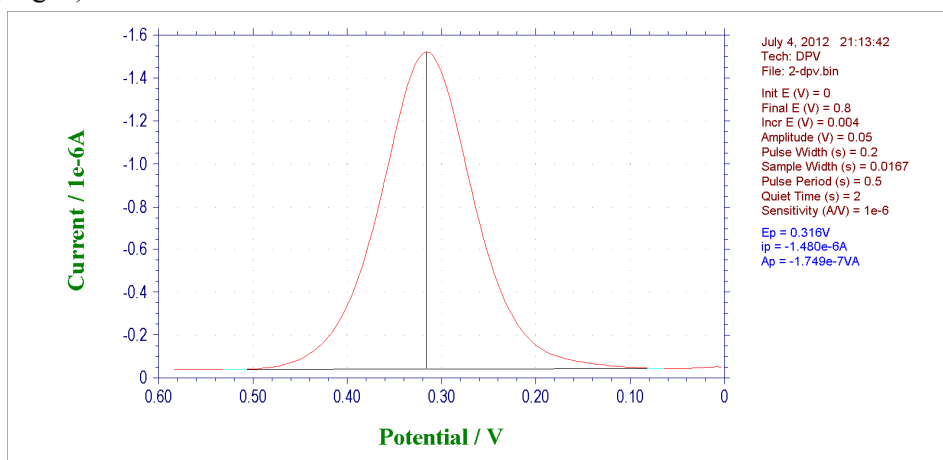


Figure S9. DPV of $\text{Mo}_2(\text{DAniF})_3(\mu\text{-O}_2\text{CC}_6\text{H}_5)$. Half-wave potential $E_p = 0.316\text{ V}$ (vs Ag/AgCl)

Table S1. Electronic coupling matrix elements from Mulliken-Hush equation.

complex	r_{ab} (Å)	r_{ab}' (Å)	E_{IT} (cm ⁻¹)	ε_{IT} (M ⁻¹ cm ⁻¹)	cal. $\Delta\nu_{1/2}$ (cm ⁻¹)	exp. $\Delta\nu_{1/2}$ (cm ⁻¹)	H_{ab} (cm ⁻¹) (r_{ab})	H_{ab} (cm ⁻¹) (r_{ab}')
[O ₂ -O ₂] ⁺	11.2	5.8	4240	1470	3190	4410	304	589
[OS-OS] ⁺	11.6	5.8	3440	3690	2820	3290	360	727
[S ₂ -S ₂] ⁺	12.2	5.8	2640	12660	2470	1770	410	864
[O ₂ -S ₂] ⁺	11.7	5.8	6560	2270	3890	4130	NA	NA

The H_{ab} values were calculated by Hush model (eq. 1). Calculated bandwidth at half-height, cal. $\Delta\nu_{1/2}$, was determined from eq. 2. Electron transfer distance r_{ab} was the [Mo₂]...[Mo₂] separation determined from the X-ray structure. Effective electron transfer distance, $r_{ab}' = 5.8$ Å, was the geometrical length of the bridging group “-CC₆H₄C-”. Spectroscopic data were extracted from the spectra of the mixed-valence complexes [Mo₂-Mo₂]⁺ as seen in Figures 1, 2, 3 and 4.

$$Hab = \frac{2.06 \times 10^{-2}}{r} (\varepsilon_{IT} \Delta \nu_{1/2} E_{IT})^{1/2} \quad (1)$$

$$cal.\Delta \nu_{1/2} = (2310 E_{IT})^{1/2} \quad (2)$$

Table S2. Effective energy gaps (ΔE_{ML}^{eff}) and effective coupling constants (H_{ML}^{eff}) for metal to ligand transition.

complex	r_{ML} (Å)	E_{ML} (cm ⁻¹)	ε_{ML} (M ⁻¹ cm ⁻¹)	$\Delta\nu_{1/2}$ (cm ⁻¹)	H_{ML} (cm ⁻¹)	ΔE_{ML}^{eff} (cm ⁻¹)	H_{ML}^{eff} (cm ⁻¹)
[O ₂ -O ₂]	5.6	20600	15230	4770	4480	18230	551
[OS-OS]	5.8	16040	25870	3580	4300	14110	655
[S ₂ -S ₂]	6.1	13850	39960	2800	4200	12390	708
[O ₂ -S ₂]	5.8	15920	22500	3290	3820	11790	618

H_{ML} values were calculated using eq. 1. H_{ML}^{eff} values were calculated by eq. 2 and ΔE_{ML}^{eff} values were calculated by eq. 3.

Electronic coupling distances (r_{ML}) are the geometrical distances determined from the X-ray structures. Spectroscopic data were extracted from the spectra of the neutral complexes [Mo₂-Mo₂].

$$H_{ML}^{eff} = \frac{H_{ML}^2}{2\Delta E_{ML}^{eff}} \quad (3)$$

$$\frac{1}{\Delta E_{ML}^{eff}} = 0.5 \times \left(\frac{1}{E_{MLCT} - E_{IT}} + \frac{1}{E_{MLCT}} \right) \quad (4)$$

Table S3. Effective energy gaps (ΔE_{LM}^{eff}) and effective coupling constants (H_{LM}^{eff}) for ligand to metal transition.

complex	r_{LM} (Å)	ε_{LM} (M ⁻¹ cm ⁻¹)	$\Delta\nu_{1/2}$ (cm ⁻¹)	E_{LM} (cm ⁻¹)	H_{LM} (cm ⁻¹)	ΔE_{LM}^{eff} (cm ⁻¹)	H_{LM}^{eff} (cm ⁻¹)
[O ₂ -O ₂] ⁺	5.6	0	0	0	0	0	0
[OS-OS] ⁺	5.8	5450	2680	12330	1500	10330	109
[S ₂ -S ₂] ⁺	6.1	17500	1350	10630	1700	9120	156
[O ₂ -S ₂] ⁺	5.8	2780	3570	12970	1260	8580	93

H_{LM} values were calculated according to eq. 1. H_{LM}^{eff} values were calculated by eq. 4 and ΔE_{LM}^{eff} values were calculated by eq. 5. Spectroscopic data were extracted from the spectra of the mixed-valence complexes [Mo₂-Mo₂]⁺. It is assumed that $r_{LM} \approx r_{ML}$ and $r_{LM'} \approx r_{ML'}$.

$$H_{LM}^{eff} = \frac{H_{LM}^2}{2\Delta E_{LM}^{eff}} \quad (5)$$

$$\frac{1}{\Delta E_{LM}^{eff}} = 0.5 \times \left(\frac{1}{E_{LMCT} - E_{IT}} + \frac{1}{E_{LM}} \right) \quad (6)$$

Table S4. Comparison between H_{ab} from Hush model and $H_{MM'}$ from CNS model.

complex	$H_{ab}(\text{cm}^{-1})^a$ ($r_{ab} = \text{Mo}_2 \cdots \text{Mo}_2$)	$H_{ab}(\text{cm}^{-1})^b$ ($r_{ab}' = 5.8 \text{ \AA}$)	H_{ML}^{eff} (cm^{-1})	H_{LM}^{eff} (cm^{-1})	$H_{MM'}$ (cm^{-1})
$[\text{O}_2\text{-O}_2]^+$	304	589	551	0	551
$[\text{OS-OS}]^+$	360	727	655	109	764
$[\text{S}_2\text{-S}_2]^+$	410	864	708	156	864
$[\text{O}_2\text{-S}_2]^+$	NA	NA	618	93	711

$H_{MM'}$ values were calculated by summation of H_{ML}^{eff} and H_{LM}^{eff} (eq. 7).

$$H_{MM'} = H_{ML}^{\text{eff}} + H_{LM}^{\text{eff}} \quad (7)$$

Table S5. Electron transfer kinetics for the symmetrical complexes based on the electronic coupling matrix elements from Hush and CNS methods.

complex	Hush			CNS		
	$\nu_{el}(\text{s}^{-1})$	ΔG^* (cm^{-1})	$k_{et}(\text{s}^{-1})$	$\nu_{el}(\text{s}^{-1})$	$\square G^*$ (cm^{-1})	$k_{et}(\text{s}^{-1})$
$[\text{O}_2\text{-O}_2]^+$	1.2×10^{14}	553	3.5×10^{11}	1.1×10^{14}	581	3.0×10^{11}
$[\text{OS-OS}]^+$	2.1×10^{14}	287	1.2×10^{12}	2.3×10^{14}	266	1.4×10^{12}
$[\text{S}_2\text{-S}_2]^+$	3.4×10^{14}	79	3.4×10^{12}	3.4×10^{14}	79	3.4×10^{12}

For the symmetrical complexes, $\lambda = E_{IT}$. The free energies of activation were calculated from eq. 7. Electronic frequencies calculated from eq. 8 are in order of 10^{14} s^{-1} and the rates of ET reactions were calculated from eq. 9, where $\kappa=1$ and $\nu_n = 5 \times 10^{12} \text{ s}^{-1}$.

$$\Delta G^* = \frac{(\lambda - 2H)^2}{4\lambda} \quad (8)$$

$$\nu_{el} = \frac{2H^2}{h} \sqrt{\frac{\pi^3}{\lambda RT}} \quad (9)$$

$$k_{et} = \kappa \nu_n \exp(-\Delta G^* / k_B T) \quad (10)$$

Table S6. Electron transfer kinetics for the unsymmetrical complexes based on the electronic coupling matrix elements from CNS methods.

complex	diabatic		adiabatic	
	ΔG^* (dia) (cm ⁻¹)	k_{et} (s ⁻¹)	$\square \Delta G^*$ (adia) (cm ⁻¹)	k_{et} (s ⁻¹)
[O ₂ -S ₂] ⁺ (forward)	2482	3.1×10^7	2430	4.1×10^7
[O ₂ -S ₂] ⁺ (reverse)	256	1.5×10^{12}	364	8.6×10^{11}

For the unsymmetrical complex, the diabatic free energies of activation (ΔG_{dia}^*) were calculated from eq.11 and the adiabatic ΔG_{adia}° and ΔG_{adia}^* were calculated using eq. 12 and 13 based on the $H_{MM'}$ derived from the CNS equations (ref. 42 in the text).

$$\Delta G^* = \frac{\lambda}{4} \left(1 + \frac{\Delta G^0}{\lambda} \right)^2 \quad (11)$$

$$\Delta G_{ad}^\circ = \Delta G^\circ \left(1 - \frac{2H_{ab}^2}{(\lambda + \Delta G^\circ)(\lambda - \Delta G^\circ)} \right) \quad (12)$$

With $\Delta G^\circ = 2226 \text{ cm}^{-1}$, $H_{ab} = 711 \text{ cm}^{-1}$ and $\lambda = 4334 \text{ cm}^{-1}$

$$\Rightarrow \Delta G_{ad}^\circ = 2063 \text{ cm}^{-1}$$

$$\Delta G^*(adia) = \frac{\lambda}{4} + \frac{\Delta G^\circ}{2} + \frac{(\Delta G^\circ)^2}{4(\lambda - 2H_{ab})} - H_{ab} + \frac{H_{ab}^2}{(\lambda + \Delta G^\circ)} \quad (13)$$